Effects of a Novel Selective PPARα Modulator, Statin, Sodium-Glucose Cotransporter 2 Inhibitor, and Combinatorial Therapy on the Liver and Vasculature of Medaka Nonalcoholic Steatohepatitis Model

Atsushi Kimura[1], Kenya Kamimura[1,2*], Marina Ohkoshi-Yamada[1], Yoko Shinagawa-Kobayashi[1], Ryo Goto[1], Takashi Owaki[1], Chiyumi Oda[1], Osamu Shibata[1], Shinichi Morita[1], Norihiro Sakai[1], Hiroyuki Abe[1], Takeshi Yokoo[1], Akira Sakamaki[1], Hiroteru Kamimura[1], Shuji Terai[1]

1. Division of Gastroenterology and Hepatology, Graduate School of Medical and Dental Sciences, Niigata University, 1-757, Aasahimachi-Dori, Chuo-Ku, Niigata, Japan

2. Department of General Medicine, Niigata University School of Medicine, 1-757, Aasahimachi-Dori, Chuo-Ku, Niigata, Japan

***Correspondence should be addressed to: Kenya Kamimura,**

Division of Gastroenterology and Hepatology

Graduate School of Medical and Dental Sciences

Niigata University

Tel: +81 (25) 227–2207

Fax: +81 (25) 227–0776

E–mail: kenya–k@med.niigata–u.ac.jp

Word count: 4,545 words

Abstract

Objective: Nonalcoholic steatohepatitis (NASH) is a disease entity with an increasing incidence, with involvement of several metabolic pathways. Various organs, including the liver, kidneys, and the vasculature, are damaged in NASH, indicating the urgent need to develop a standard therapy. Therefore, this study was conducted to investigate the effects of drugs targeting various metabolic pathways and their combinations on a high-fat diet (HFD)-induced NASH medaka model.

Methods: To investigate the effects of drugs on vascular structures, the NASH animal model was developed using the *fli::GFP* transgenic medaka fed with HFD at 20 mg/fish daily. The physiological changes, histological changes in the liver, vascular structures in the fin, and serum biochemical markers were evaluated in a time-dependent manner after treatment with selective peroxisome proliferator-activated receptor α modulator (pemafibrate), statin (pitavastatin), sodium-glucose cotransporter 2 inhibitor (tofogliflozin), and their combinations. Furthermore, to determine the mechanisms underlying the effects, whole transcriptome sequencing was conducted using medaka liver samples.

Results: Histological analyses revealed significant suppression of fat accumulation and fibrotic changes in the liver after treatment with drugs and their combinations. The expression levels of steatosis- and fibrosis-related genes were modified by the treatments. Moreover, the HFD-induced vascular damages in the fin exhibited milder changes after treatment with the drugs.

Conclusion: The effects of treating various metabolic pathways on the medaka body, liver, and vascular structures of the NASH medaka model were evidenced. Moreover, to our knowledge, this study is the first to report whole genome sequence and gene expression evaluation of medaka livers, which could be helpful in clarifying the molecular mechanisms of drugs.

Keywords: NASH; *fli::GFP* transgenic medaka; SPPARMα; statin; SGLT2 inhibitor

Introduction

Nonalcoholic fatty liver disease (NAFLD) is closely associated with metabolic dysregulation, including obesity, diabetes, hyperlipidemia, hypertension, and insulin resistance and it is frequently complicated with various metabolic complications of cardiovascular events and chronic kidney disease [1]. Therefore, it is reasonable to hypothesize that therapeutic interventions for metabolic dysregulation could reverse hepatic steatosis and slow down the liver inflammation and fibrosis in NASH [2]. Although various studies have demonstrated the potential of each target, no standard therapeutic option has been established as a successful regimen to date. Therefore, we have examined the effect of selective peroxisome proliferator-activated receptor α modulator (SPPARMα) of pemafibrate (PEMA) [3]; the statin of pitavastatin (PITA) that is known to decrease hepatic inflammation through the inhibition of RhoA and Ras signaling [4, 5]; the sodium-glucose cotransporter 2 inhibitor (SGLT2I) of tofogliflozin (TOFO), which reduce hyperglycemia and NAFLD and its cardiovascular events [6]; and the combinations of these drugs on NASH and its vascular damages in medaka NASH model [7-9] in this study.

Materials and Methods

Animals and diets

All animal experiments were conducted in full compliance with the regulations of the

Institutional Animal Care and Use Committee at Niigata University (Niigata, Japan) that also approved the study protocol (Nos. 406-6, 00424, and 00804). All animals received humane care according to the criteria outlined in the "Guide for the Care and Use of Laboratory Animals" prepared by the National Academy of Sciences (USA). *fli*::*GFP* transgenic medaka (Strain ID: TG1206) was supplied by NBRP Medaka (https://shigen.nig.ac.jp/medaka/), in which a GFP-expressing cassette was inserted under the control of the *fli* promoter of Kyoto-Cab strain and drives gene expression in all blood vessels in the fish [7]. The fish used in the experiments were aged 6 months. They were maintained in plastic tanks containing 2 L of tap water under fluorescent light from 8 AM to 8 PM. The water temperature was maintained at 25°C ± 1°C. The medaka NASH model was developed by feeding the medaka fish with a high-fat diet (HFD, HFD32; CLEA Japan, Tokyo, Japan) using a previously reported method [8-10]. Briefly, each tank was supplied with a control diet or an HFD at 20 mg/fish daily, with all the provided food being consumed within 14 h. The energy content of the control standard diet was 3.8 kcal/g, with 23.2% of calories being derived from fat, 44.0% from protein, and 32.7% from carbohydrate; vitamins and minerals were provided as recommended (Hikari labo M-450; Kyorin Co. Ltd, Hyogo, Japan). Every 7–8 medakas at each four time points for the six groups of HFD, HFD + pemafibrate (PEMA), HFD + tofogliflozin (TOFO), HFD + pitavastatin (PITA), HFD + PEMA + TOFO, and HFD + PITA + TOFO were prepared and analyzed, i.e., >40 medakas for each time point. Results were confirmed by repeating three times each

experiment; therefore, approximately 480 medakas were evaluated.

Drug administration

PEMA, TOFO, and PITA (Kowa Co. Ltd., Tokyo, Japan) were dissolved in dimethyl sulfoxide to maintain the concentration of the drugs in the water tanks (Nacalai Tesque, Kyoto, Japan). The final concentration of PEMA was 6 μg/L, which is similar to the Cmax of 6 ng/mL for humans treated with the dose of 0.4 mg used in clinical trial for NAFLD (ClinicalTrials.gov, number: NCT03350165) [11]. The final concentration of TOFO was 0.5 mg/L, which is similar to the Cmax of 500 ng/ml for humans treated with the standard dose of 20 mg. The final concentration of PITA was 0.056 mg/L, which is similar to the Cmax of 26 ng/ml for humans treated with the standard dose of 2 mg. For the combinatorial dosage of PEMA + TOFO and PITA + TOFO, the dose adjusted below the abovementioned concentration was prepared in the tank. This determination of concentration in the tank is consistent with our previous studies conducted using telmisartan, TOFO, and sorafenib in a medaka model [7-9, 12]. The same amount of dimethyl sulfoxide was administered to the tank of the HFD group. The water, HFD, and drug in the tank were replaced every 2 days, and the tanks were carefully washed to maintain a consistent concentration.

Histological analyses

Liver tissue samples were collected at the appropriate time points, fixed in 10% formalin, and embedded in paraffin. Sections (10-μm-thick) were stained with standard hematoxylin and eosin (HE) or Sirius red. Hepatocyte fat deposition in the liver was detected by HE staining, and fibrotic tissue in the liver was detected as the area stained red by Sirius red staining. Then, the images were captured randomly from each tissue section, and a quantitative analysis of fat deposition areas and fibrotic areas was performed using the ImageJ software (version 1.8.0_112, National Institutes of Health, USA) with the RGB-based protocol as reported previously [13].

Whole transcriptome sequencing

Whole transcriptome sequencing of *Oryzias latipes* (Japanese medaka) was performed to investigate the different gene expression profiles and to perform gene annotation on a set of useful genes based on gene ontology pathway information (outsourced to Macrogen Japan Corp. Koto City, Tokyo, Japan). Detailed information was shown in **Information of the Supplementary Materials**.)

RT-PCR

For reverse transcription PCR (RT-PCR), total RNA was extracted from the liver tissue using the RNeasy Mini kit (QIAGEN, Hilden, Germany) and reverse-transcribed into cDNA using the QuantiTect Reverse Transcription Kit (QIAGEN). The gene expression levels were

measured by PCR using Taq DNA polymerase (Applied Biosystems AmpliTaq Gold) (MiniAmp Plus Thermal Cycler, WAKENYAKU, Kyoto, Japan). These reactions were analyzed in a microchip electrophoresis system (MCE-202 MultiNA; Shimadzu, Kyoto, Japan) using the DNA-1000 Reagent Kit. Using the MultiNA Viewer software, the band shades of each product were represented as the peak area, quantified, and compared respectively. The thermal conditions were as follows: 94°C for 10 min, followed by 40 cycles of 94°C for 30 s, 55°C for 30 s, 72°C for 1 min, 72°C for 7 min, and 4°C. The primers used in this experiment were *Gapdh* [14], *Col1a1a*, *Mmp2*, *Timp2b*, *Tgfb1* [15], *Acc1*, *Fas*, *Pparγ* [12], and *Pparα* [16] (Sigma–Aldrich, Tokyo, Japan) and summarized in **Supplementary Table 1**.

Analysis of vasculature in the medaka model

The vascular structure of *fli*::*GFP* medaka was evaluated using a fluorescence stereomicroscope (BZ-X800; Keyence Corporation, Osaka, Japan), and images were quantitatively analyzed using the ImageJ software (version 1.8.0_112, National Institutes of Health, USA), as reported previously [13]. A region of interest (ROI) of 20 × 100 μm^2 was used to determine the vascular area in the ROI when the vascular structure was placed at the center of the ROI.

Statistical analyses

The obtained data were analyzed using either the Student's *t*-test or a two-way factor repeated-measures analysis of variance (ANOVA), followed by Tukey's multiple comparison test. $p < 0.05$ was considered to indicate statistical significance.

Results

Effects of drugs on body and liver weights of HFD-fed fli::GFP transgenic medaka

The medaka NASH model was developed by feeding *fli::GFP* transgenic medaka with HFD as reported previously [10] to investigate the effects of the drugs PEMA, TOFO, PITA, PEMA + TOFO, and PITA + TOFO on NASH **(Figure 1A)**. Time-dependent macroscopic changes in the livers of HFD-fed medaka treated or untreated with drugs for 12 weeks are shown in **Figure 1B**. The HFD-fed medaka showed a time-dependent increase in body weight (BW) and liver weight (LW), peaking at 8 weeks of HFD feeding **(Figure 1C)**. Although no significant changes were observed in LW, the tendency to inhibit LW gain was observed in the drug-treated groups at 8 weeks, and the LW/BW ratio was significantly suppressed at 12 weeks after treatment with PEMA, PEMA + TOFO, or PITA + TOFO **(Figure 1C)**.

Effects of drugs on the liver tissue of medaka

As the time-dependent and significant progression of hepatic steatosis and fibrosis were evident by HE staining and Sirius red staining at 12 weeks in the HFD-fed *fli::GFP* transgenic medaka, the effects of drugs on these histological changes in HFD-fed medaka were examined **(Figure**

2). Although PITA and PITA + TOFO retarded the hepatic steatosis 4 and 8 weeks after HFD feeding **(Figure 2A, B)**, PEMA resulted in long-term suppression of hepatic steatosis after 12 weeks of HFD feeding ($p < 0.05$), and its effect was further increased when combined with TOFO **(**PEMA + TOFO, $p < 0.001$, **Figure 2A, 2B)**. Sirius red staining demonstrated a continuous effect of PEMA on the suppression of liver fibrosis progression by 12 weeks and TOFO at 8 and 12 weeks after HFD feeding **(Figure 2C, D)**, and further suppression was observed with PEMA + TOFO and PITA + TOFO at 12 weeks after HFD feeding. These results suggest that PEMA is effective in reducing steatosis and fibrosis in the liver and its effect increases in the later stage when combined with TOFO.

Effects of drugs on gene expression in the liver of medaka

Whole transcriptome sequencing was performed as mentioned earlier, and to determine the effect of the drugs on the medaka NASH model, the changes in the expression of various genes in liver cells were examined by transcriptome sequencing **(Figure 3)**. Analyses were successfully performed on all seven paired-end samples **(Supplementary Figure 1A)**. **Supplementary Figure 1B** shows the throughput of raw data and trimmed data, and **Supplementary Figure 1C** shows the Q30 percentage (% of bases with quality over phred score 30) of each sample's raw and trimmed data. Then, DEG analysis was performed on six comparison pairs of normal liver vs HFD12W, PITA4W vs HFD12W, PEMA8W vs HFD12W,

TOFO8W vs HFD12W, PEMA + TOFO12W vs HFD12W, and PITA + TOFO vs HFD12W, which revealed significant differences in histological analyses, using edgeR to determine the potential mechanisms underlying the reduction of hepatic steatosis and fibrosis by these drugs. The results disclosed 3720 genes that satisfied |fc|≥2 & exactTest raw $p < 0.05$ conditions in at least one of comparison pairs. **Figure 3A** and **3B** shows the result of hierarchical clustering (distance metric = Euclidean distance, linkage method = complete) analysis. It graphically represents the similarity of expression patterns between samples and genes. The DEG list was further analyzed in gProfiler (https://biit.cs.ut.ee/gprofiler/orth) for gene set enrichment analysis per biological process (BP), cellular component (CC), and molecular function (MF); **Figure 3C–E** shows the significant gene set according to each category. Other than the significant changes in the gene expression categorized in BP in the group treated with PITA **(Figure 3C)** and PEMA **(Figure 3C)** and in CC in the group treated with TOFO **(Figure 3D)**, genes related to MF exhibited significant changes in groups treated with 4WPITA, 8WPEMA, 8WTOFO, and 12WPEMA + TOFO, and 12WPITA + TOFO in a time-dependent manner **(Figure 3E)**. Each set of these categories in the comparisons is shown in **Supplementary Figure 2**.

To further determine the effects of drugs on the liver, the genes related to steatosis and fibrosis that exhibited significant differences in RNA-Seq analyses were evaluated in the liver by RT-

PCR **(Figure 3F and 3G)**. Among the 3720 genes that exhibited significant differences in expression in at least one comparison **(Figure 3A)**, the genes of acetyl-CoA carboxylase 1 (*Acc1*), 5.7-fold FC decrease in normal liver, fatty acid synthase (*Fas*), 57-fold FC decrease in normal liver, 3.6- and 116-fold decrease in PEMA + TOFO12W and PITA + TOFO12W, respectively, peroxisome proliferator-activated receptor alpha (*Pparα*), 2.2- and 4.3-fold FC increase in PEMA8W and TOFO8W, peroxisome proliferator-activated receptor gamma (*Pparγ*), 3.0-fold FC decrease in TOFO8W, collagen type I, alpha 1a (*col1a1a*), 5.1-fold FC decrease in normal liver, 4.7-fold decrease in PITA + TOFO12W group, matrix metalloproteinase 2 (*Mmp2*), 5.2-, 2.9-, and 4.6-fold FC decrease in normal liver, PITA4W, and PEMA + TOFO12W, tissue inhibitors of metalloproteinase 2b (*Timp2b*) showed 4.5-, 3.6-, and 3.4-fold FC increase in normal liver, PEMA + TOFO12W, and PITA + TOFO12W, respectively, and transforming growth factor beta 1 (*Tgfβ1*), 2.3-, 2.7-, 2.1-, and 2.1-fold FC decreases in normal liver, PEMA8W, TOFO8W, and PEMA + TOFO12W, respectively, were evaluated for each time point. Based on the results, *Acc1* and *Pparγ* expression showed significant inhibition in groups treated with PEMA, TOFO, and PEMA + TOFO at 8 weeks, and *Fas* expression showed a decreasing tendency in groups treated with PEMA and TOFO at 4 and 8 weeks. *Pparα* expression showed no significant changes **(Figure 3F)**. Furthermore, PEMA- and TOFO-treated groups showed decreased expression of *Col1a1a* at 4 weeks and of *Timp2b* and *Tgfβ1* at 8 weeks, and the PITA-treated group showed inhibition of *Mmp2*, *Timp2b*, and *Tgfβ1*

expression after 8 weeks. Moreover, the combinatorial medication of PEMA + TOFO and PITA + TOFO resulted in suppression of these fibrosis-related gene expressions continuously by 12 weeks of HFD feeding. These results indicate that the gene expression changes caused by these drugs could contribute to the suppression of the HFD-induced hepatic steatosis and fibrosis, especially in the PEMA- and TOFO-group at 8 weeks that led to the histological differences observed at 12 weeks.

Effects of drugs on the vascular structures of HFD-fed medaka fin

As *Pparγ* has been reported to be the key molecule for the promotion of adipogenesis [17], which is related to atherosclerosis of vessels [18], the vascular structures in the fin of HFD-fed medaka were examined after treatment with the drugs **(Figure 4)**. The HFD-fed *fli::GFP* transgenic medaka fish showed narrowing changes in the vascular diameter due to the atherosclerotic changes that led to a decrease in the GFP-positive area in the fin after 12 weeks of HFD feeding **(Figure 4A)**, which was significantly different **(Figure 4B)**. The medaka fish treated with the drugs showed maintenance of the vascular area at 12 weeks after HFD feeding, especially when treated with the regimens comprising PEMA (PEMA, PEMA + TOFO) **(Figure 4B)**.

Effects of drugs on biochemical parameters

Although the levels of TG, ALT, γGTP, TC, LDL-C, HDL-C, and BS showed a decreasing tendency after treatment with the drugs, the differences were not statistically significant **(Supplementary Figure 3)**.

Discussion

Although there is no standard therapeutic option for NASH, because it is generally considered as a hepatic manifestation of metabolic syndrome, the development of strategies to address metabolic dysregulation is a foundational element for therapeutic options [1]. Accordingly, our study demonstrated that the progression of NAFLD pathology was controlled by PEMA, TOFO, and PITA, and their combinations by various degrees as evidenced by biochemical analyses, histological analyses, gene expression analyses, and vasculature analysis in the HFD-fed medaka fish (*O. latipes*) model. Among the drugs, PEMA and PEMA + TOFO resulted in a suppressive effect on LW/BW, hepatic steatosis, and fibrosis, and PITA had an effect on steatosis, LW/BW, and fibrosis when combined with TOFO **(Figure 1)**. Furthermore, these drugs, especially PEMA, PITA, and their combinations with TOFO, resulted in milder atherosclerotic changes in vascular diameter **(Figure 4)**. The underlying mechanisms included modifications of the gene expression of steatosis-related *Acc1* and *Pparγ* when treated with PEMA, TOFO, and their combination. PPARs are nuclear receptors that play a regulatory role in lipid metabolism and considered as key drugs for treating NASH and its cardiovascular

complications [3]. Among them, PEMA decreases serum TG levels, increases HDL-C levels, and improves NASH pathogenesis through the modulation of lipid turnover and energy metabolism in the liver [3, 11] and exerts a beneficial effect in ischemic vascular diseases [19]. Statins improves liver function and reduce the cardiovascular events of NAFLD cases [5] while the fewer reports on PITA have been reported due to concerns of hepatotoxicity [20]. SGLT2 inhibitors reduce hyperglycemia by suppressing glucose reabsorption in the proximal tubules and improving insulin resistance, glucotoxicity, and lipotoxicity [21]. They have been shown to be effective in ameliorating NAFLD progression in basic [8, 22] and clinical [23] studies. Furthermore, SGLT2 inhibitors have the potential of cardiorenal protection [24]. Among them, TOFO is a highly specific SGLT2 inhibitor [25] that reduces hyperglycemia and NAFLD and its cardiovascular events [6]. We had recently demonstrated that TOFO exerts effect on fatty infiltration and fibrotic changes in the liver [8] and on the renal injury [9] of HFD-fed medaka NASH model. To further consider the effective treatment for NASH and its complications in the vascular structures, we combined these therapeutic agents to target several metabolic pathways and showed its efficacy. The combinatorial effects have not been reported to date other than the report combining thiazolidinedione and liraglutide [26], which showed improved glucose tolerance and liver histology, and combining apical sodium-bile acid transporter inhibitor and fibroblast growth factor-15 signaling activation, which improved NASH pathology [27].

Medaka has been used to for NAFLD studies [8, 16] and the *fli::GFP* transgenic medaka model used in the current study is useful for determining the cardiovascular lumen as it expresses GFP in vascular endothelial cells [28] and for examining the vascular damage by detecting the GFP-positive area in their fins [7]. Our study might have a limitation in serum biochemical analyses because the total blood volume that can be collected from a medaka is approximately 2 μL, and therefore, the blood samples collected from all animals from the three repeated experiments were pooled and measured as a single sample, and hence, the result was not accurate.

In conclusion, the effects of SPPARMα, statin, and SGLT2 inhibitor on the liver and vascular structure of the medaka NASH model were evidenced. Furthermore, the HFD-induced *fli::GFP* transgenic medaka NASH model was useful for determining the effects on the liver, the vascular structures, and the gene expression in the liver to clarify the molecular mechanisms of the action of drugs.

Figure Legends

Figure 1. Effects of drugs on macroscopic findings and the body and liver weights of HFD-fed *fli::GFP* transgenic medaka

(A). Schematic presentation of the study design. (B). Time-dependent macroscopic changes in the medaka body. (C). Liver weight (LW) and body weight (BW) were calculated at the appropriate time points. The values represent mean ± SD (n = 15 for each group). * $p < 0.05$ compared to HFD group. Two-way ANOVA followed by Bonferroni's multiple comparison test. The scale bar represents 5 mm. HFD, high-fat diet, PEMA, pemafibrate, TOFO, tofogliflozin, PITA, pitavastatin, BL, body length, BW, body weight, LW, liver weight. Hr, heart; Lv, liver; GB, gall bladder; Gut, digestive tract.

Figure 2. Effects of drugs on histological changes and deposition of fatty and fibrotic tissue in the liver of HFD-fed *fli::GFP* transgenic medaka

(A) Representative microscopic findings of medaka liver tissues stained with hematoxylin and eosin. **(B)** Quantitative analysis of fat deposition areas in the medaka liver. **(C)** Representative microscopic findings of medaka liver tissues stained with Sirius red. **(D)** Quantitative analysis of the fibrotic area in the medaka liver. Scale bar represents 100 μm. The values represent mean ± SD (n = 15 for each group). * $p < 0.05$, ** $p < 0.01$, and *** $p < 0.001$ compared to HFD group. Student's *t*-test.

Figure 3. Effects of drugs on gene expression in the liver of HFD-fed *fli::GFP* transgenic medaka

(A) Heatmap for differentially expressed genes. **(B)** Hierarchical clustering. **(C)** Gene set enrichment analysis per biological process, **(D)** cellular component (CC), **(E)** molecular function (MF). **(F)** Expression of hepatic steatosis-related genes in each animal group. *Acc1*, acetyl-CoA carboxylase 1, *Fas*, fatty acid synthase, *Pparα*, peroxisome proliferator-activated receptor alpha, *Pparγ*, peroxisome proliferator-activated receptor gamma, *Gapdh*, Glyceraldehyde 3-phosphate dehydrogenase. **(G)** Expression of hepatic fibrosis-related genes in each animal group. *Col1a1a*, collagen type I, alpha 1a, *Mmp2*, matrix metalloproteinase 2, *Timp2b*, tissue inhibitors of metalloproteinase 2b, *Tgfβ1*, transforming growth factor beta. The values represent mean ± SD (n = 5). *$p < 0.05$, **$p < 0.01$, and N.S., no statistical significance. Student's *t*-test.

Figure 4. Effects of drugs on the vascular structures of HFD-fed *fli*::*GFP* transgenic medaka

(A) GFP-positive area in the fin. (B) GFP-positive vascular area in the region of interest (ROI) of 20 × 100 μm^2. The values represent mean ± SD (three vessels each in six medakas in each

group were evaluated) * $p < 0.05$, ** $p < 0.01$, and N.S., no statistical significance. Student's *t*-test.

References

1. R. Loomba, SL. Friedman, GI Shulman. Mechanisms and disease consequences of nonalcoholic fatty liver disease. *Cell* **184**: 2537-2564, 2021.
2. Y. Sumida, M. Yoneda. Current and future pharmacological therapies for NAFLD/NASH. *J Gastroenterol.* **53**: 362-376, 2018.
3. Y. Honda, T. Kessoku, Y. Ogawa, et al. Pemafibrate, a novel selective peroxisome proliferator-activated receptor alpha modulator, improves the pathogenesis in a rodent model of nonalcoholic steatohepatitis. *Sci Rep* **7**: 42477, 2017.
4. R. Schierwagen, L. Maybüchen, K. Hittatiya, et al. Statins improve NASH via inhibition of RhoA and Ras. *Am J Physiol Gastrointest Liver Physiol* **311**: G724-G733, 2016.
5. H Hyogo, T Ikegami, K. Tokushige, et al. Efficacy of pitavastatin for the treatment of non-alcoholic steatohepatitis with dyslipidemia: An open-label, pilot study. *Hepatol Res* **41**: 1057-1065, 2011.
6. M. Yoneda, Y. Honda, Y. Ogawa, et al. Comparing the effects of tofogliflozin and pioglitazone in non-alcoholic fatty liver disease patients with type 2 diabetes mellitus (ToPiND study): a randomized prospective open-label controlled trial. *BMJ Open Diabetes Res Care* **9**: e001990, 2021.
7. Y. Shinagawa-Kobayashi, K. Kamimura, R. Goto, et al. Effect of histidine on sorafenib-induced vascular damage: Analysis using novel medaka fish model. *Biochem Biophys Res Commun.* **496**: 556-561, 2018.
8. R. Goto, K. Kamimura, Y. Shinagawa-Kobayashi, et al. Inhibition of sodium glucose cotransporter 2 (SGLT2) delays liver fibrosis in a medaka model of nonalcoholic steatohepatitis (NASH). *FEBS Open Bio* **9**: 643-652, 2019.
9. T. Nagoya, K. Kamimura, R. Goto, et al. Inhibition of sodium-glucose cotransporter 2 ameliorates renal injury in a novel medaka model of nonalcoholic steatohepatitis-related kidney disease. *FEBS Open Bio* **9**: 2016-2024, 2019.

10. T. Matsumoto, S. Terai, T. Oishi, et al. Medaka as a model for human nonalcoholic steatohepatitis. *Dis Model Mech.* **3**: 431-440, 2010.
11. A. Nakajima, Y. Eguchi, M. Yoneda, et al. Randomised clinical trial: Pemafibrate, a novel selective peroxisome proliferator-activated receptor α modulator (SPPARMα), versus placebo in patients with non-alcoholic fatty liver disease. *Aliment Pharmacol Ther*., 2021 Epub ahead of print.
12. S. Kuwashiro, S. Terai, T. Oishi, et al. Telmisartan improves nonalcoholic steatohepatitis in medaka (Oryzias latipes) by reducing macrophage infiltration and fat accumulation. *Cell Tissue Res.* **344**: 125-134, 2011.
13. T. Vrekoussis, V. Chaniotis, I. Navrozoglou, et al. Image analysis of breast cancer immunohistochemistry-stained sections using ImageJ: an RGB-based model. *Anticancer Res.* **29**: 4995-4998, 2009.
14. F. Mao, S. Keita, K. Mai, et al. Comparison of stress response between two wild populations of Japanese medaka, Oryzias latipes and O. sakaizumii *Nippon Suisan Gakkaishi* **80**: 379-381, 2014.
15. AJ. Van Wettere, JM. Law, DE. Hinton, et al. Anchoring hepatic gene expression with development of fibrosis and neoplasia in a toxicant-induced fish model of liver injury. *Toxicol Pathol* **41**: 744-760, 2013.
16. S. Raza-Iqbal, T. Tanaka, M. Anai, et al. Transcriptome Analysis of K-877 (a Novel Selective PPARα Modulator (SPPARMα))-regulated genes in primary human hepatocytes and the mouse liver. *J Atheroscler Thromb* **22**: 754-772, 2015.
17. Y. Tonoyama, M. Tsukada, Y. Imai, et al. Establishment of a quantitative in vivo method for estimating adipose tissue volumes and the effects of dietary soy sauce oil on adipogenesis in medaka, Oryzias latipes. *PLoS One* **13**: e0205888, 2018.
18. G. Fantuzzi, T. Mazzone. Adipose tissue and atherosclerosis: exploring the connection. *Arterioscler Thromb Vasc Biol* **27**: 996-1003, 2007.

19. H. Kawanishi, K. Ohashi, H. Ogawa, et al. A novel selective PPARα modulator, pemafibrate promotes ischemia-induced revascularization through the eNOS-dependent mechanisms. *PLoS One* **15**: e0235362, 2020.

20. MJ. Thomson, M. Serper, V. Khungar, et al. Prevalence and factors associated with statin use among patients with nonalcoholic fatty liver disease in the TARGET-NASH Study. *Clin Gastroenterol Hepatol*., 2021 Epub ahead of print.

21. A. Tahara, T. Takasu, M. Yokono, et al. Characterization and comparison of sodium-glucose cotransporter 2 inhibitors in pharmacokinetics, pharmacodynamics, and pharmacologic effects. *J Pharmacol Sci.* **130**: 159-169, 2016.

22. A. Obata, N. Kubota, T. Kubota, et al. Tofogliflozin improves insulin resistance in skeletal muscle and accelerates lipolysis in adipose tissue in male mice. *Endocrinology.* **157**: 1029-1042, 2016.

23. D. Ito, S. Shimizu, K. Inoue, et al. Comparison of Ipragliflozin and Pioglitazone effects on nonalcoholic fatty liver disease in patients with type 2 diabetes: A randomized, 24-Week, open-label, active-controlled trial. *Diabetes Care.* **40**: 1364-1372, 2017.

24. B. Neal, V. Perkovic, KW. Mahaffey, et al. Canagliflozin and Cardiovascular and Renal Events in Type 2 Diabetes. *N Engl J Med* **377**: 644-657, 2017.

25. M. Suzuki, K. Honda, M. Fukazawa, et al. Tofogliflozin, a potent and highly specific sodium/glucose cotransporter 2 inhibitor, improves glycemic control in diabetic rats and mice. *J Pharmacol Exp Ther*. **341**: 692-701, 2012.

26. DR. Kamm, KD. Pyles, MC. Sharpe, et al. Novel insulin sensitizer MSDC-0602K improves insulinemia and fatty liver disease in mice, alone and in combination with liraglutide. *J Biol Chem.* **296**: 100807, 2021.

27. DJ. Matye, H. Wang, W. Luo, et al. Combined ASBT inhibitor and FGF15 treatment improves therapeutic efficacy in experimental non-alcoholic steatohepatitis. *Cell Mol Gastroenterol Hepatol*. **12**: 1001-1019, 2021.

28. N. Mittal, SH. Yoon, H. Enomoto, et al. Versican is crucial for the initiation of cardiovascular lumen development in medaka (Oryzias latipes). *Sci Rep* **9**: 9475, 2019.

Acknowledgments

The authors would like to thank Takao Tsuchida in the Division of Gastroenterology and Hepatology at the Niigata University for his excellent assistance in the histological analyses. The authors would also like to thank Nobuyoshi Fujisawa, Kanako Oda, Shuko Adachi, Katsuya Hirasawa, Takenori Sakuma, Toshikuni Sasaoka, and all staff members at the Division of Laboratory Animal Resources in Niigata University.

Conflicts of interests

The authors declare that they have no competing interests.

Funding

The research in the authors' laboratories has been supported in part by a Grant-in-Aid for Scientific Research from the Japanese Society for the Promotion of Sciences 25670370, 16K15424, and 18K19537 to Terai S and Kamimura K. And this work was partly supported by Kowa Co., Ltd.. The funders had no role in study design, data collection and analysis, decision to publish or preparation of the manuscript

Graphical Abstract

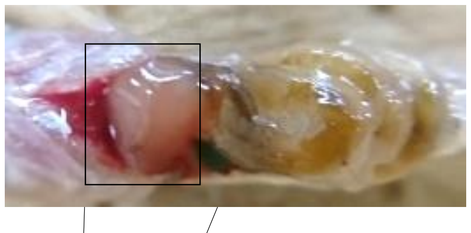

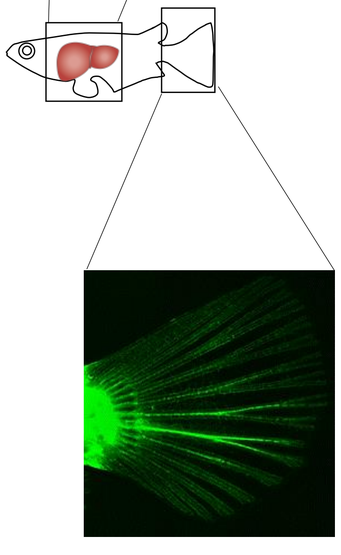

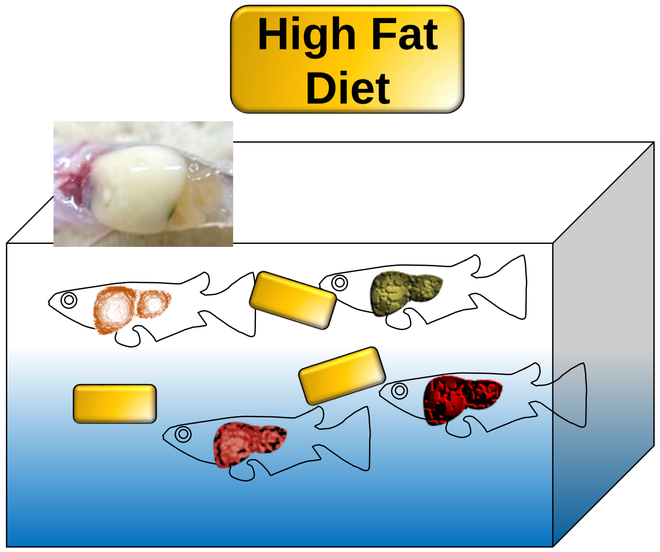

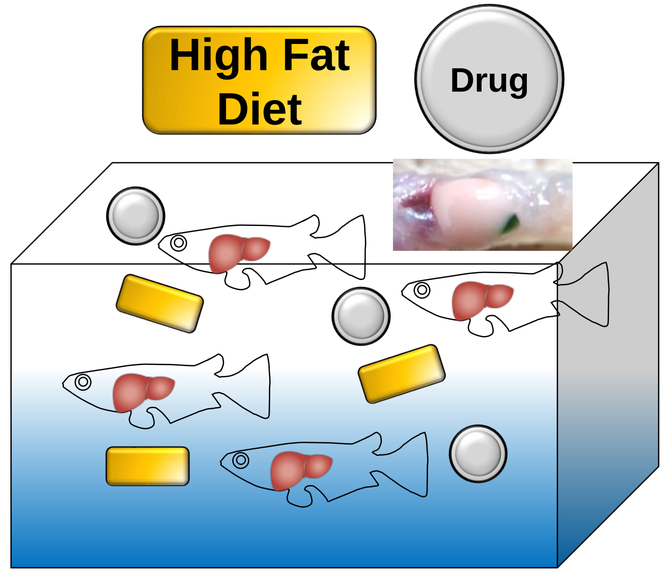

HFD-induced Liver Damage

Fatty Liver

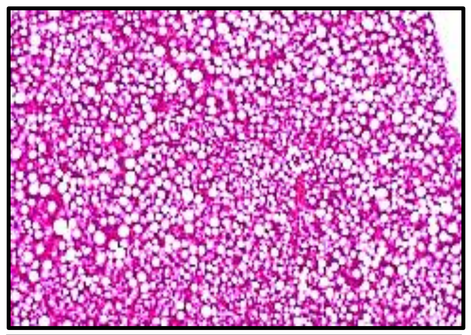

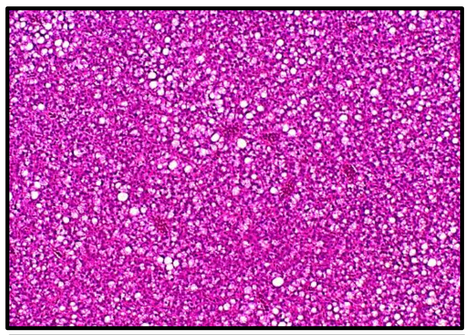

Liver Fibrosis

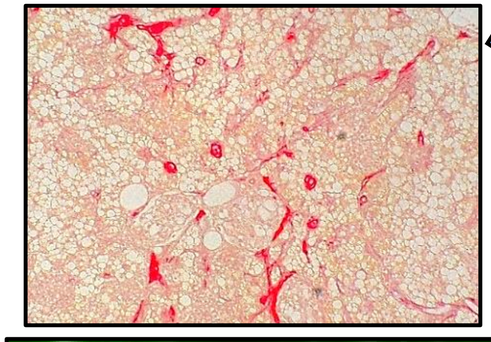

Amelioration

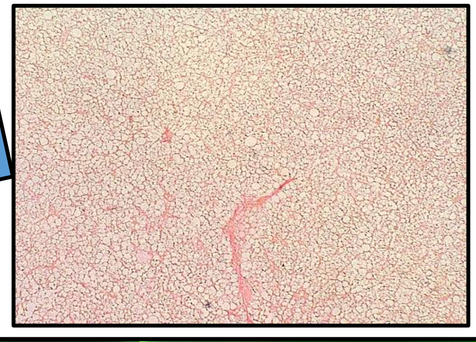

HFD-induced Vascular Damage

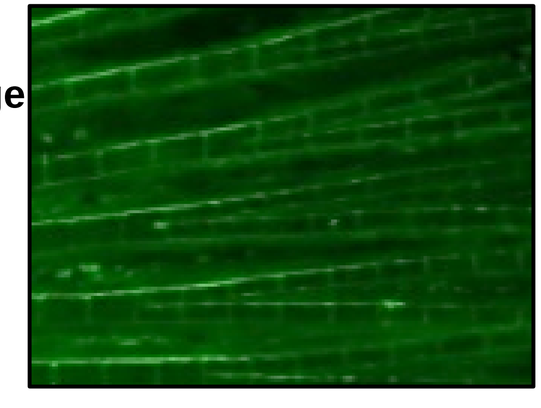

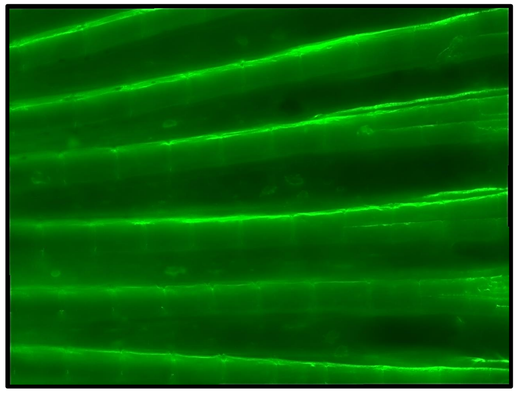

Figure 1

(A)

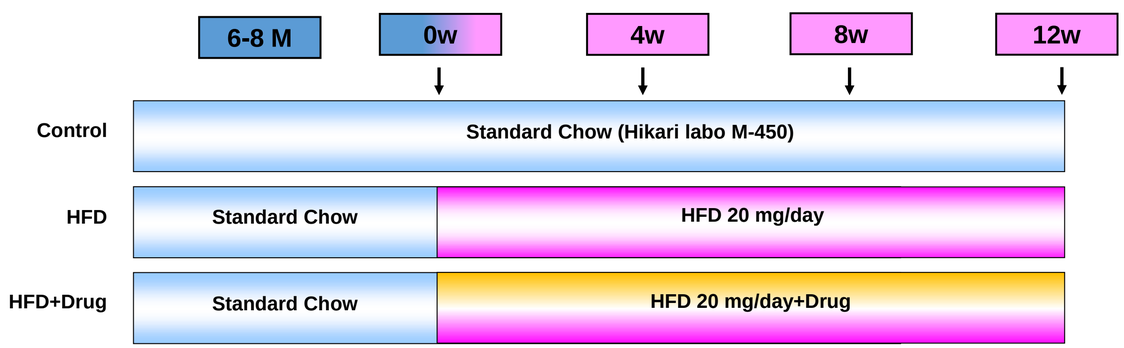

Group	HFD	Drug
Control	- (Standard Chow)	-
HFD	+	-
HFD+PEMA	+	PEMA (6 μg/L)
HFD+TOFO	+	TOFO (0.5 mg/L)
HFD+PITA	+	PITA (0.056 mg/L)
HFD+PEMA+TOFO	+	PEMA (6 μg/L)+TOFO (0.5 mg/L)
HFD+PITA+TOFO	+	PITA (0.056 mg/L)+TOFO (0.5 mg/L)

(B)

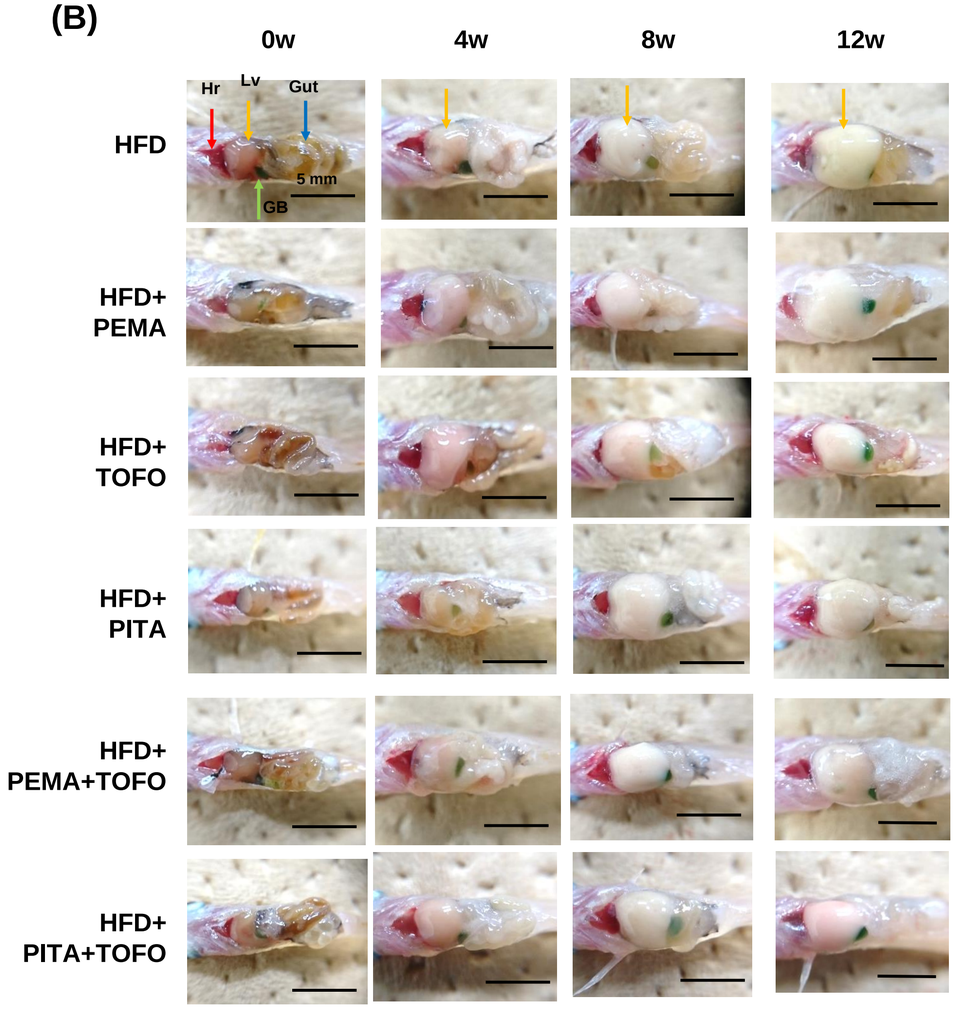

(C)

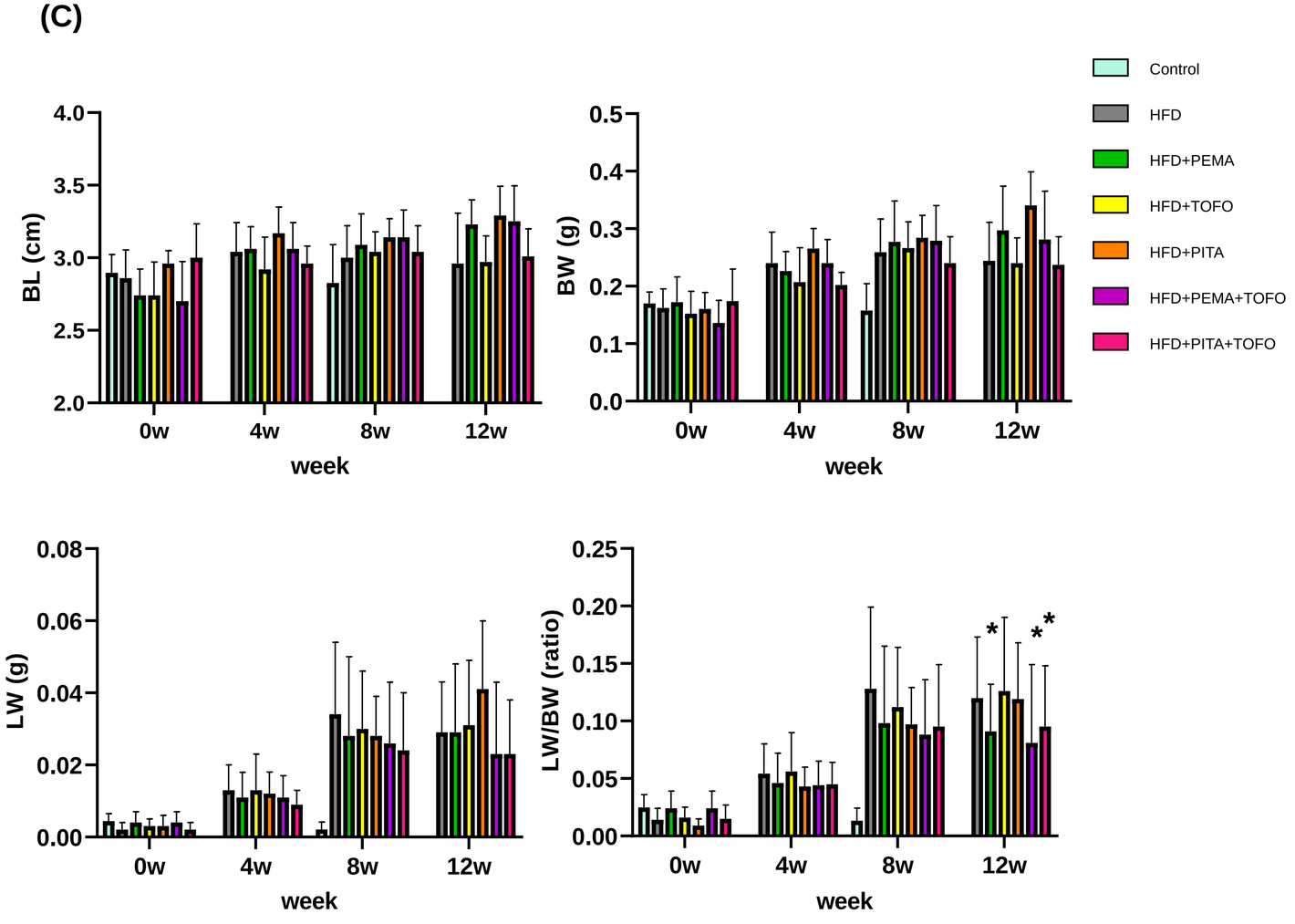

Figure 2

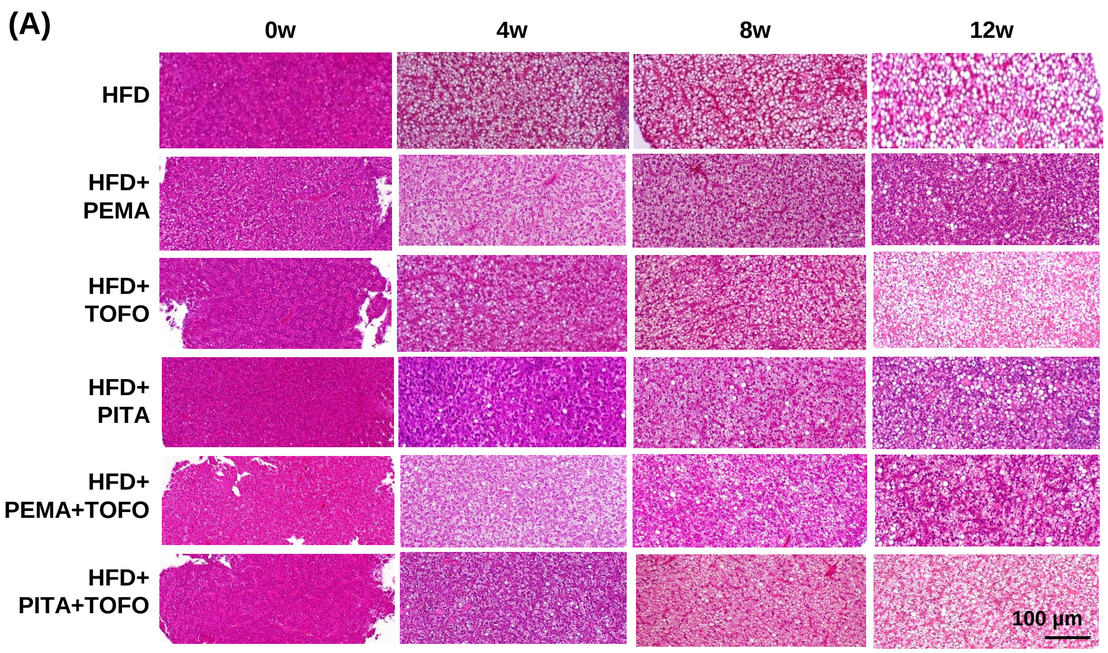
(A)
0w
4w
8w
12w
HFD
HFD+ PEMA
HFD+ TOFO
HFD+ PITA
HFD+ PEMA+TOFO
HFD+ PITA+TOFO
100 μm

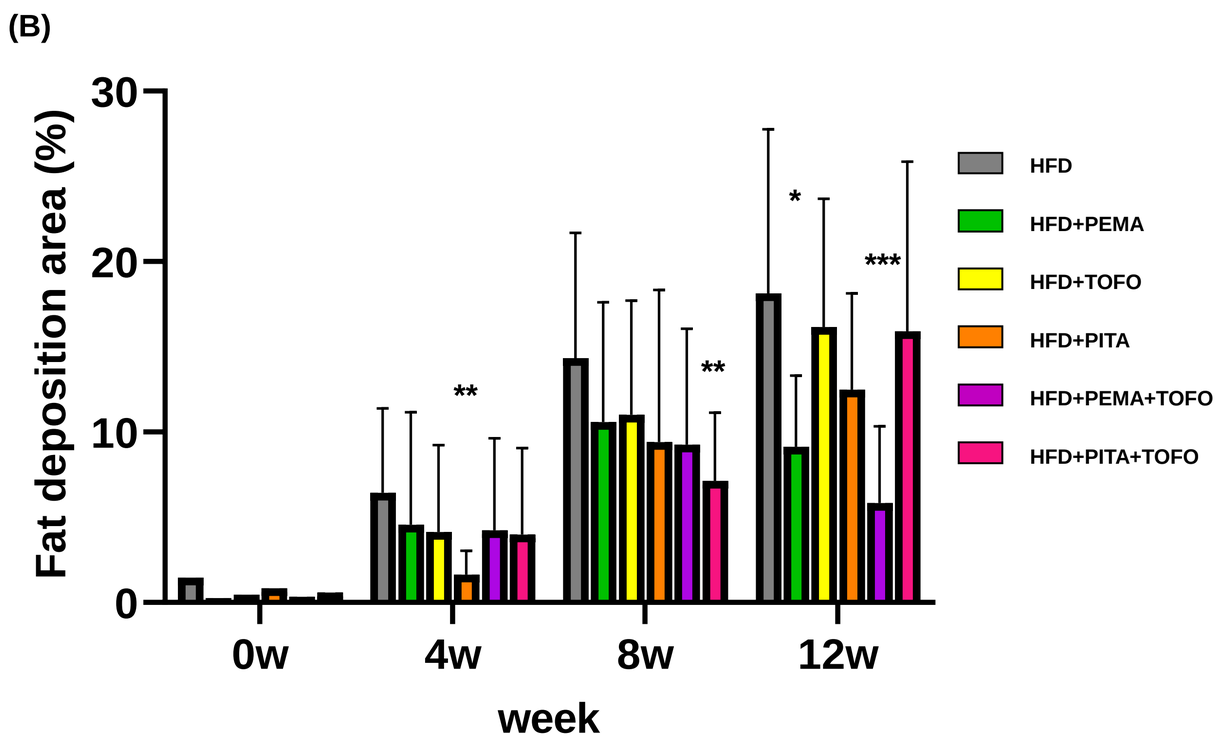
(B)
Fat deposition area (%)
30
20
10
0
0w
4w
8w
12w
week
HFD
HFD+PEMA
HFD+TOFO
HFD+PITA
HFD+PEMA+TOFO
HFD+PITA+TOFO

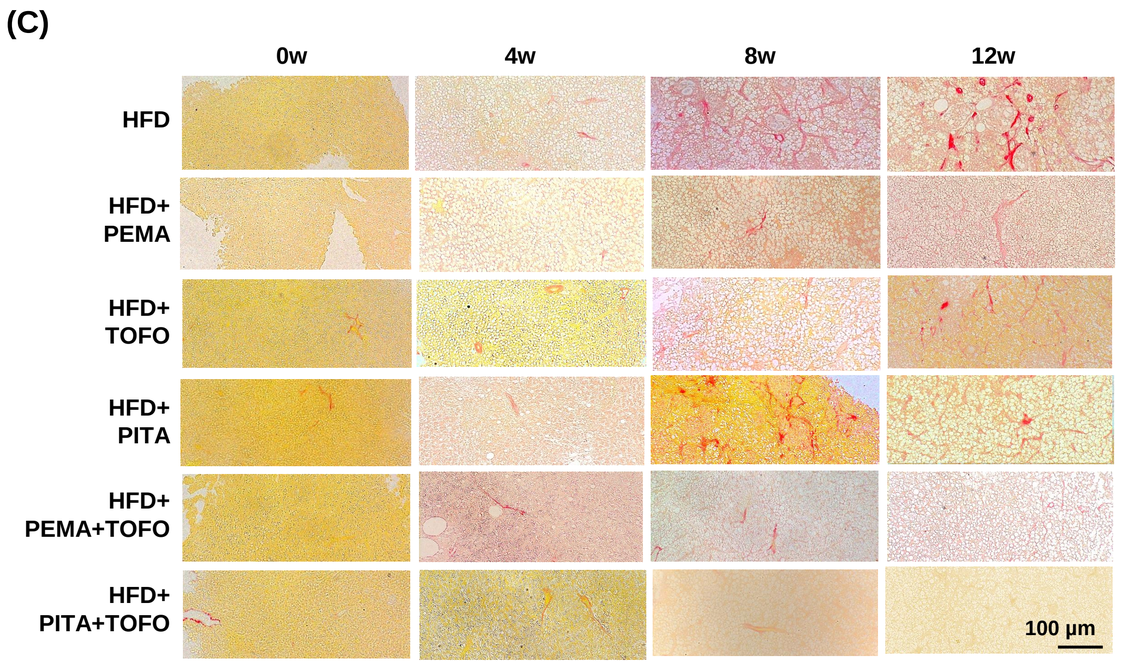
(C)
0w
4w
8w
12w
HFD
HFD+ PEMA
HFD+ TOFO
HFD+ PITA
HFD+ PEMA+TOFO
HFD+ PITA+TOFO
100 μm

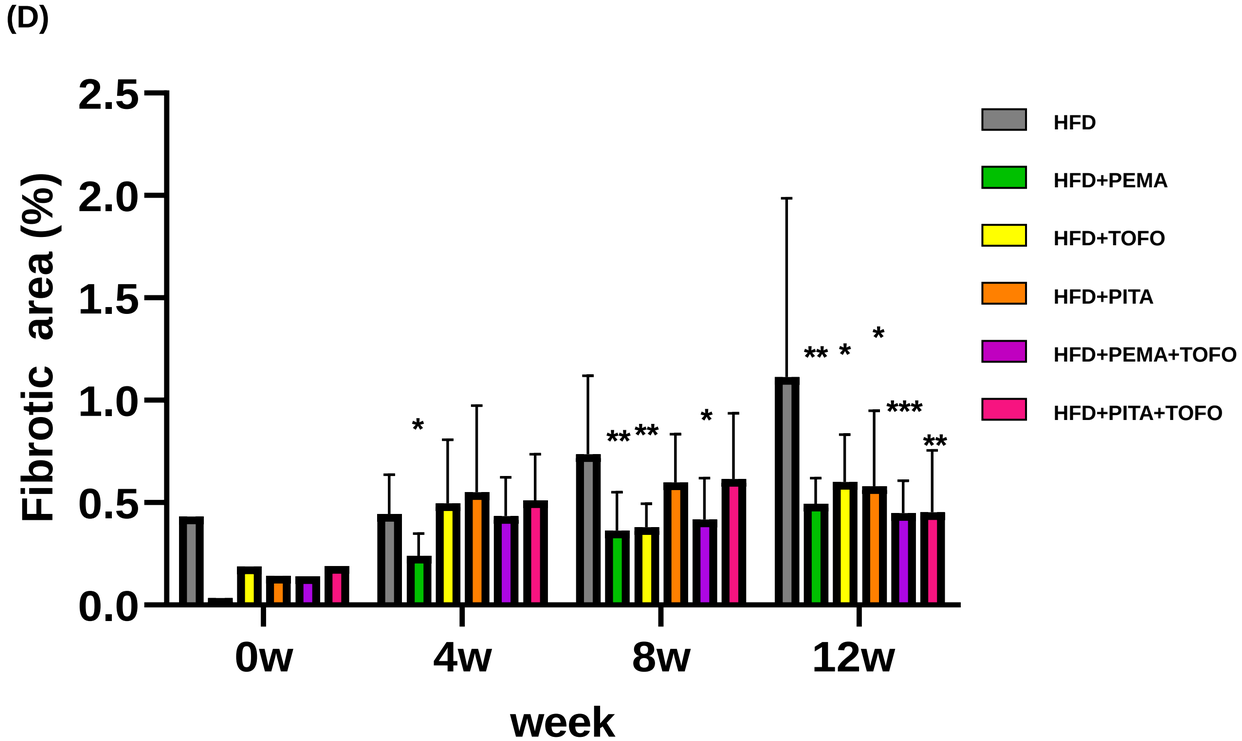
(D)
Fibrotic area (%)
2.5
2.0
1.5
1.0
0.5
0.0
0w
4w
8w
12w
week
HFD
HFD+PEMA
HFD+TOFO
HFD+PITA
HFD+PEMA+TOFO
HFD+PITA+TOFO

Figure 3

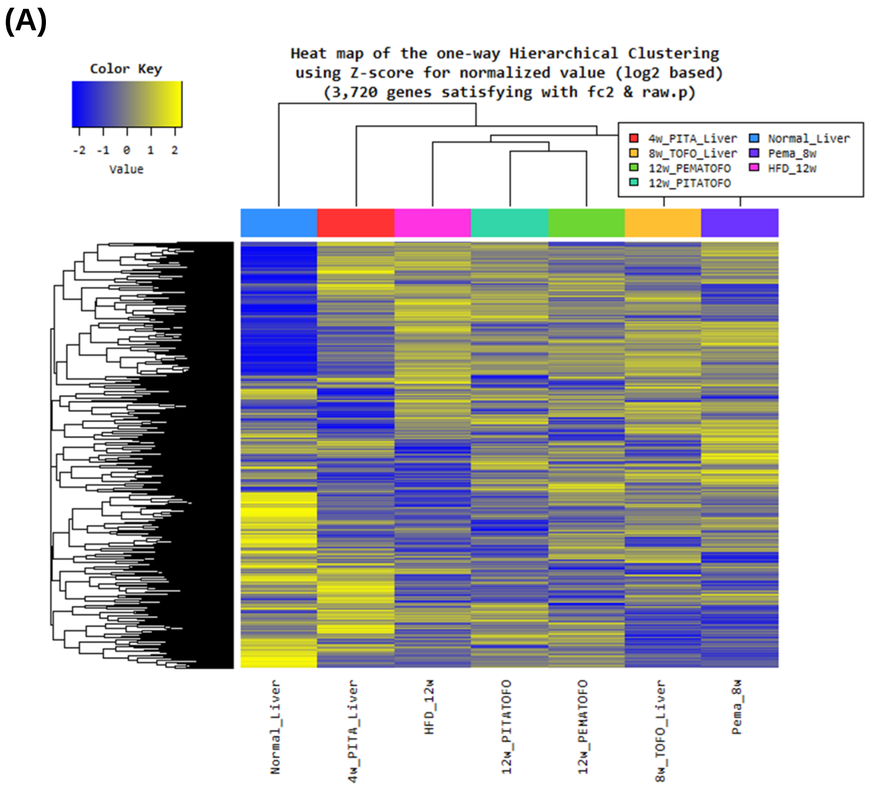
(A)
Heat map of the one-way Hierarchical Clustering
using Z-score for normalized value (log2 based)
(3,720 genes satisfying with fc2 & raw.p)
Color Key
-2 -1 0 1 2
Value
4w_PITA_Liver
8w_TOFO_Liver
12w_PEMATOFO
12w_PITATOFO
Normal_Liver
Pema_8w
HFD_12w
Normal_Liver
4w_PITA_Liver
HFD_12w
12w_PITATOFO
12w_PEMATOFO
8w_TOFO_Liver
Pema_8w

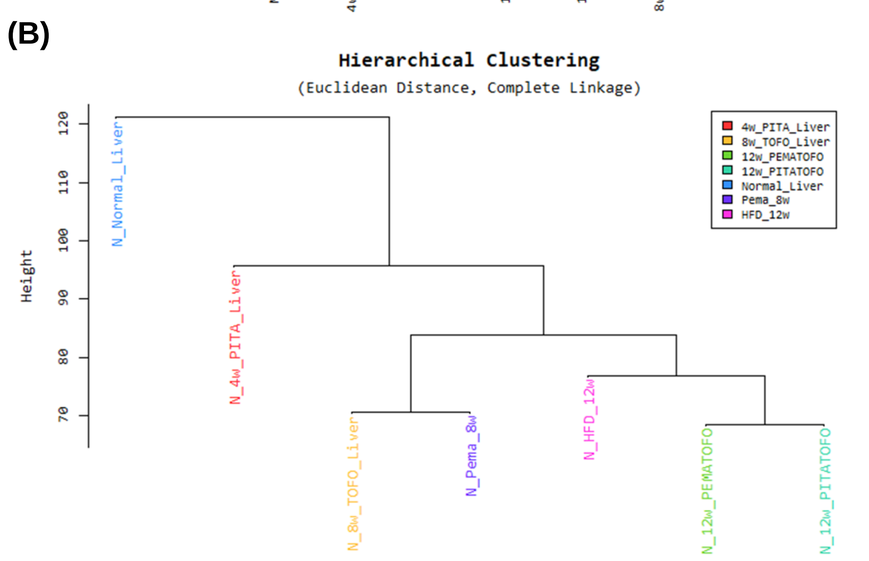
(B)
Hierarchical Clustering
(Euclidean Distance, Complete Linkage)
Height
120
110
100
90
80
70
N_Normal_Liver
N_4w_PITA_Liver
N_8w_TOFO_Liver
N_Pema_8w
N_HFD_12w
N_12w_PEMATOFO
N_12w_PITATOFO
4w_PITA_Liver
8w_TOFO_Liver
12w_PEMATOFO
12w_PITATOFO
Normal_Liver
Pema_8w
HFD_12w

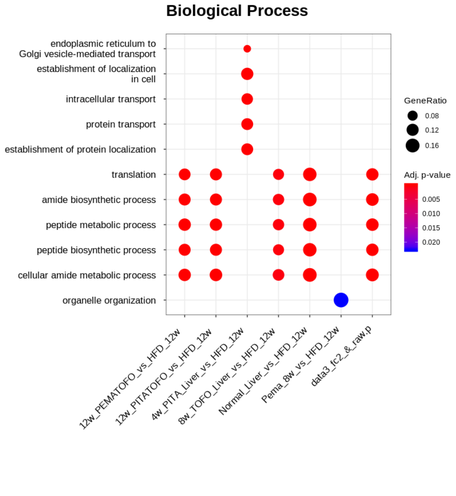
(C)
Biological Process
endoplasmic reticulum to Golgi vesicle-mediated transport
establishment of localization in cell
intracellular transport
protein transport
establishment of protein localization
translation
amide biosynthetic process
peptide metabolic process
peptide biosynthetic process
cellular amide metabolic process
organelle organization
GeneRatio
0.08
0.12
0.16
Adj. p-value
0.005
0.010
0.015
0.020
12w_PEMATOFO_vs_HFD_12w
12w_PITATOFO_vs_HFD_12w
4w_PITA_Liver_vs_HFD_12w
8w_TOFO_Liver_vs_HFD_12w
Normal_Liver_vs_HFD_12w
Pema_8w_vs_HFD_12w
data3_fc2_&_raw.p

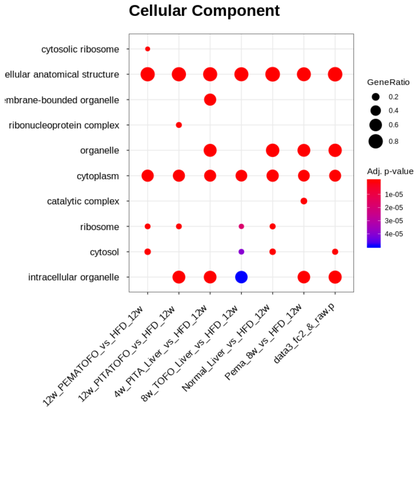
(D)
Cellular Component
cytosolic ribosome
ellular anatomical structure
mbrane-bounded organelle
ribonucleoprotein complex
organelle
cytoplasm
catalytic complex
ribosome
cytosol
intracellular organelle
GeneRatio
0.2
0.4
0.6
0.8
Adj. p-value
1e-05
2e-05
3e-05
4e-05
12w_PEMATOFO_vs_HFD_12w
12w_PITATOFO_vs_HFD_12w
4w_PITA_Liver_vs_HFD_12w
8w_TOFO_Liver_vs_HFD_12w
Normal_Liver_vs_HFD_12w
Pema_8w_vs_HFD_12w
data3_fc2_&_raw.p

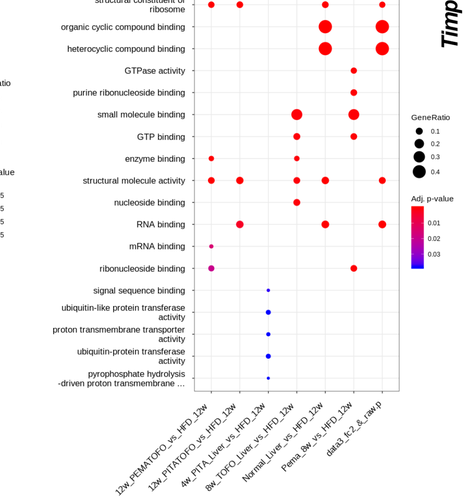
(E)
Molecular Function
structural constituent of ribosome
organic cyclic compound binding
heterocyclic compound binding
GTPase activity
purine ribonucleoside binding
small molecule binding
GTP binding
enzyme binding
structural molecule activity
nucleoside binding
RNA binding
mRNA binding
ribonucleoside binding
signal sequence binding
ubiquitin-like protein transferase activity
proton transmembrane transporter activity
ubiquitin-protein transferase activity
pyrophosphate hydrolysis -driven proton transmembrane ...
GeneRatio
0.1
0.2
0.3
0.4
Adj. p-value
0.01
0.02
0.03
12w_PEMATOFO_vs_HFD_12w
12w_PITATOFO_vs_HFD_12w
4w_PITA_Liver_vs_HFD_12w
8w_TOFO_Liver_vs_HFD_12w
Normal_Liver_vs_HFD_12w
Pema_8w_vs_HFD_12w
data3_fc2_&_raw.p

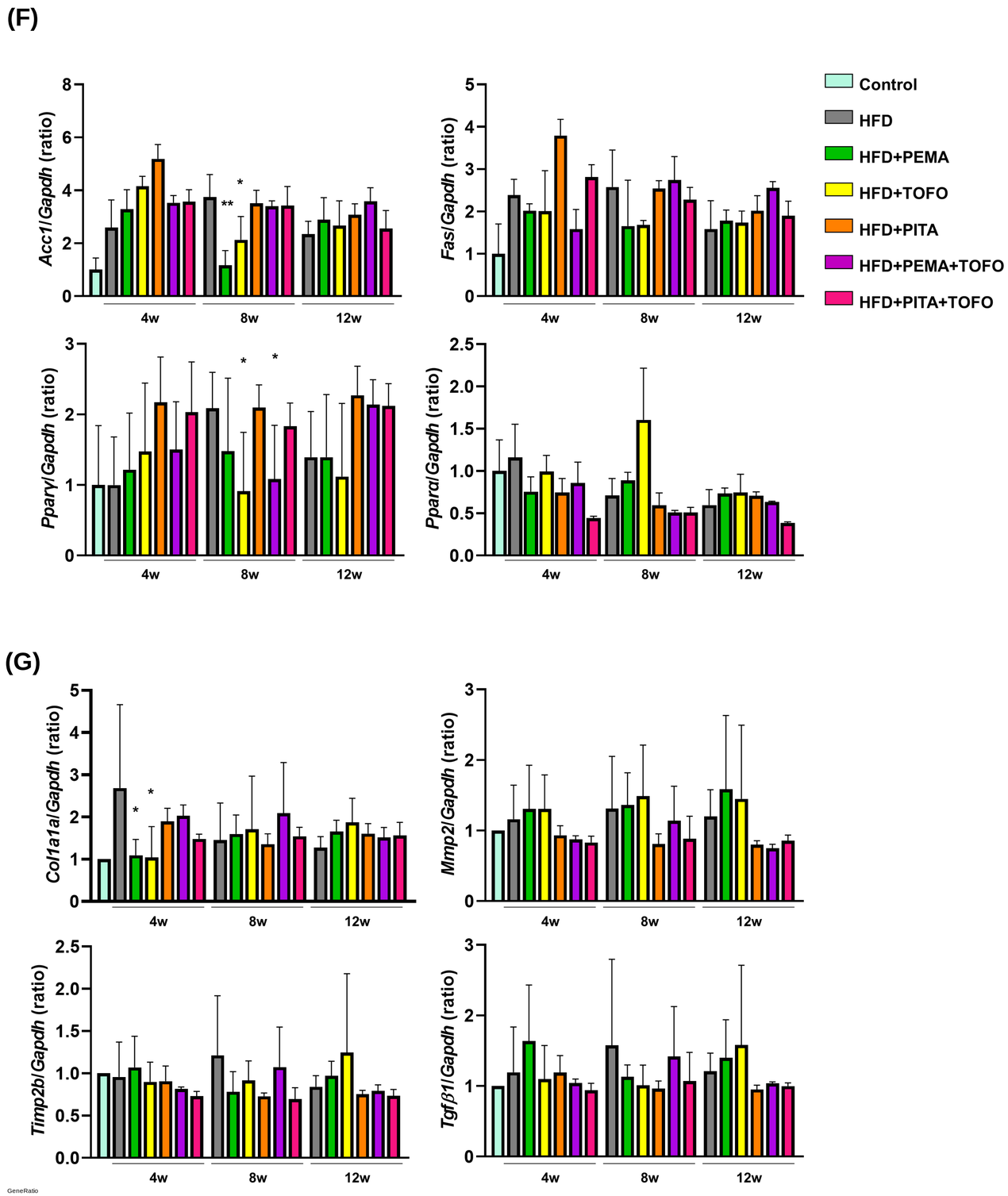
(F)
Acc1/Gapdh (ratio)
Fas/Gapdh (ratio)
Pparγ/Gapdh (ratio)
Pparα/Gapdh (ratio)
4w
8w
12w
Control
HFD
HFD+PEMA
HFD+TOFO
HFD+PITA
HFD+PEMA+TOFO
HFD+PITA+TOFO
(G)
Col1a1a/Gapdh (ratio)
Mmp2/Gapdh (ratio)
Timp2b/Gapdh (ratio)
Tgfβ1/Gapdh (ratio)

Figure 4

(A)

Chow-fed Medaka

HFD-fed Medaka

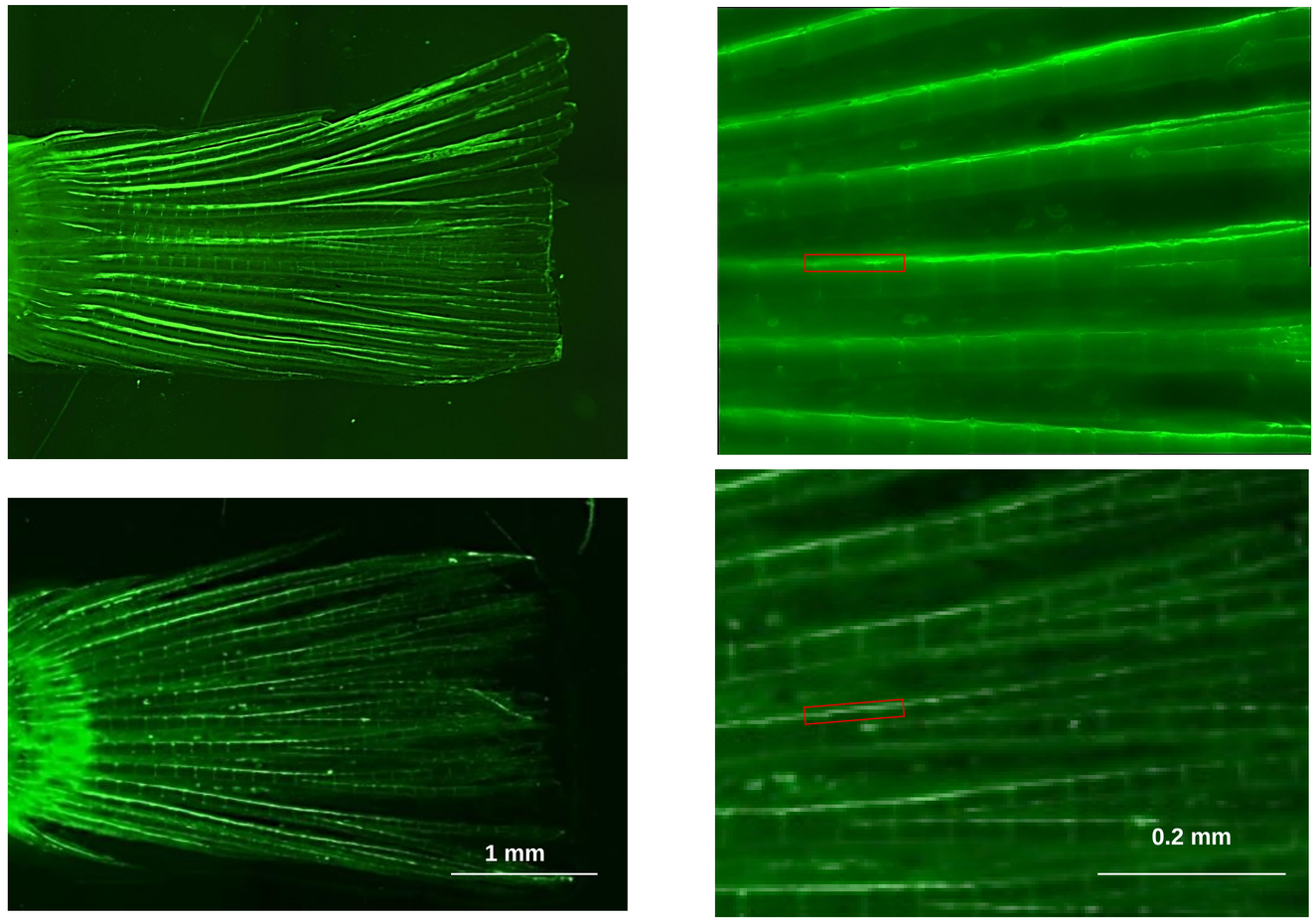

(B)

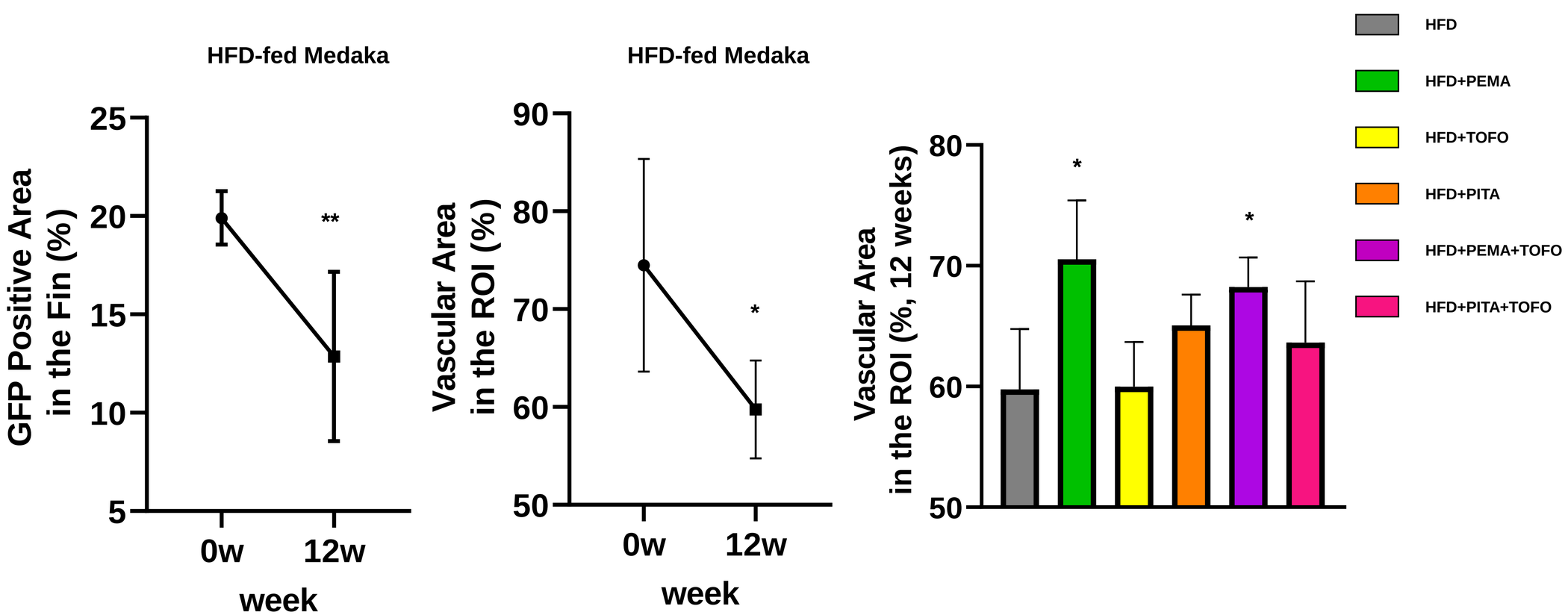

Supplementary Figure 1

(A)

Index	Sample id	Total read bases*	Total reads	GC (%)	Q20 (%)	Q30 (%)
1	4w_PITA_Liver	6,336,619,002	62,738,802	44.80	98.26	95.09
2	8w_TOFO_Liver	6,324,527,080	62,619,080	67.32	98.83	96.53
3	12w_PEMATOFO	6,310,778,960	62,482,960	65.28	98.76	96.46
4	12w_PITATOFO	6,299,032,862	62,366,662	59.08	98.67	96.05
5	HFD_12w	6,310,961,164	62,484,764	57.23	98.59	96.01
6	Normal_Liver	6,365,039,594	63,020,194	70.15	98.94	96.74
7	Pema_8w	5,519,062,988	54,644,188	57.02	98.82	96.56

(B)

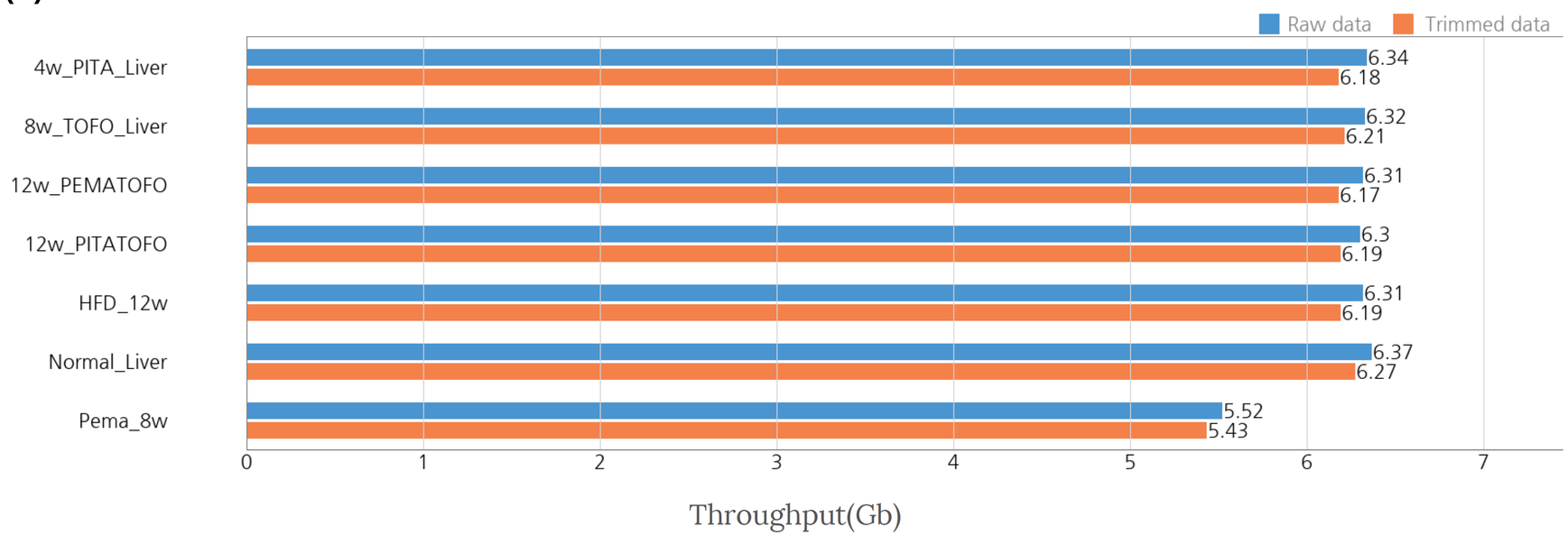

(C)

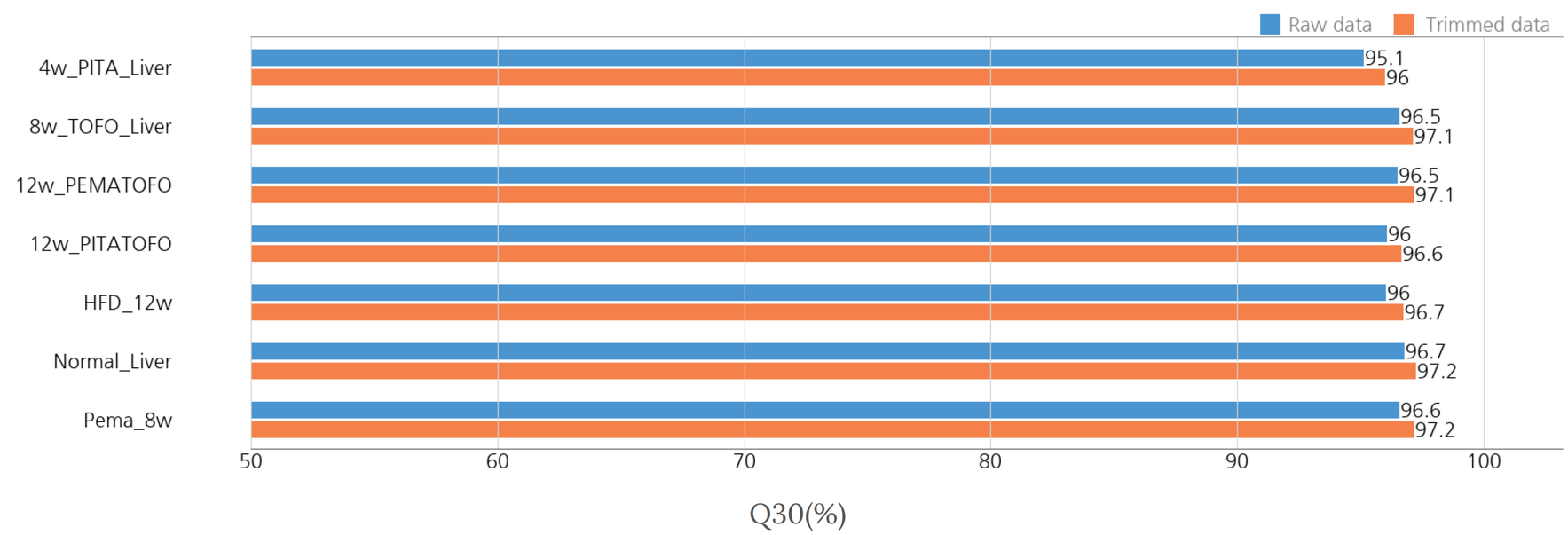

Supplementary Figure 2

Normal vs HFD 12W

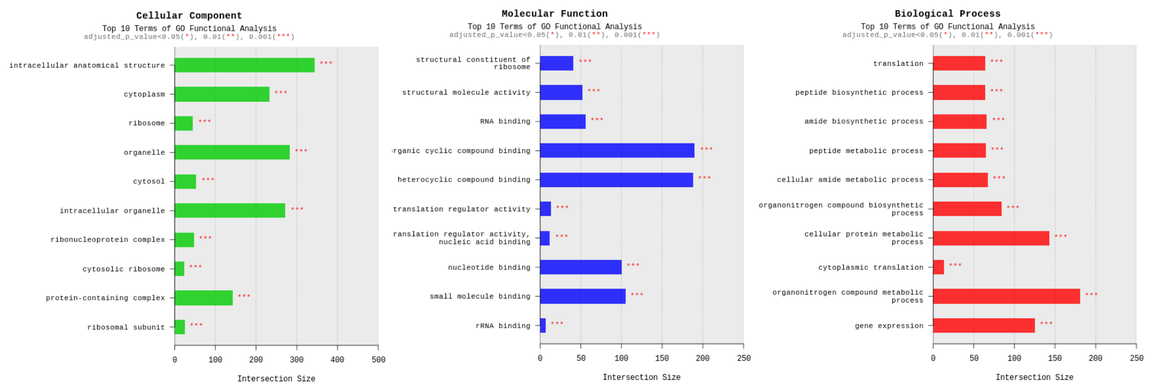

PITA4W vs HFD 12W

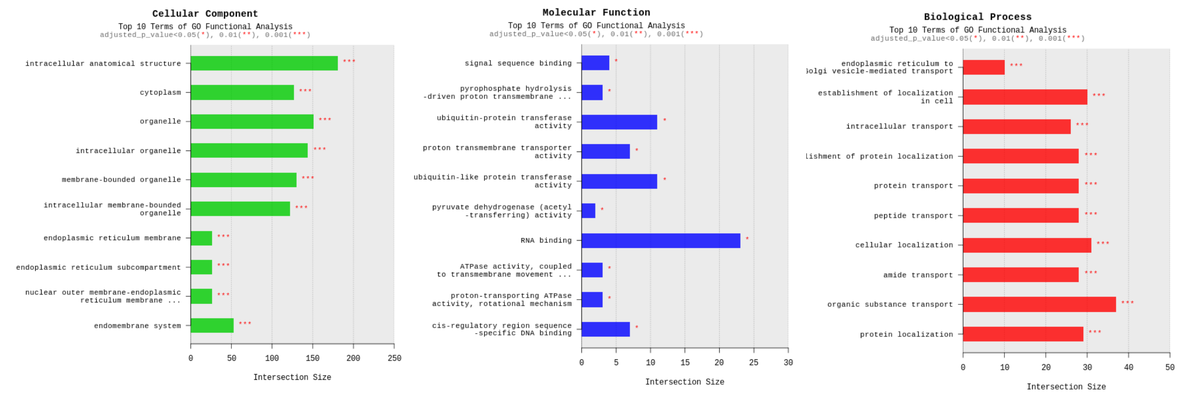

PEMA8W vs HFD 12W

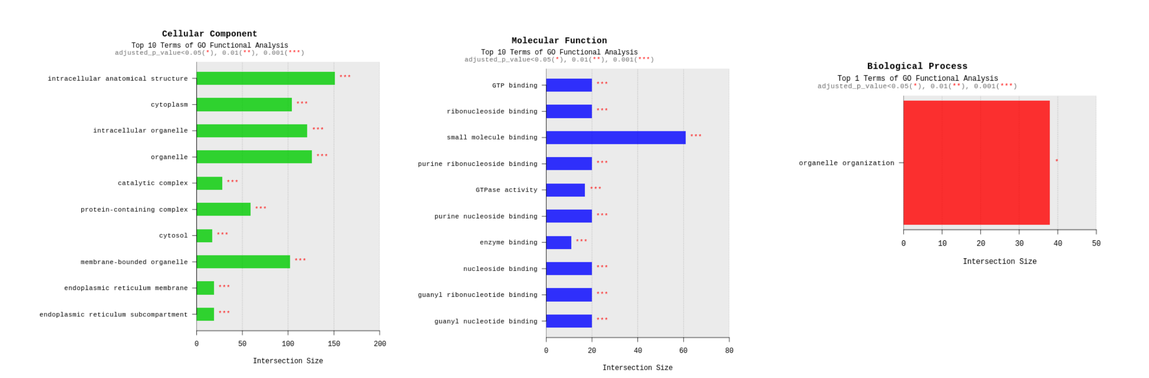

PEMA+TOFO12W vs HFD 12W

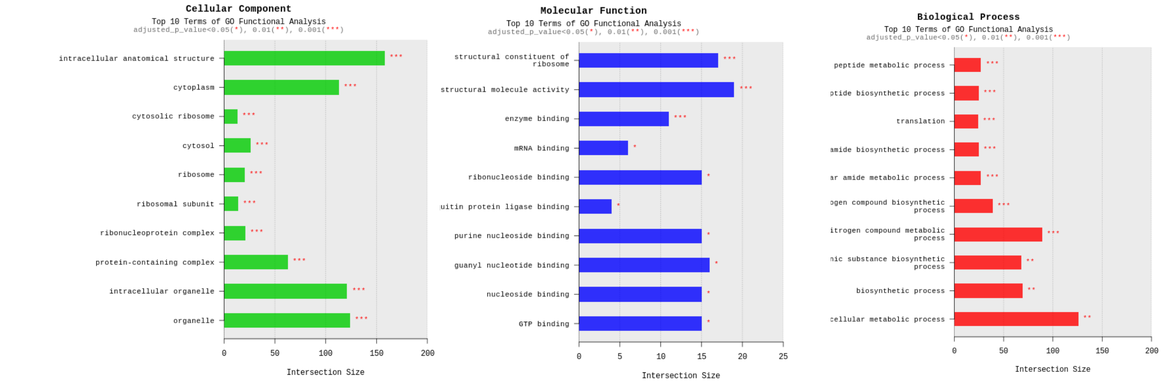

TOFO8W vs HFD 12W

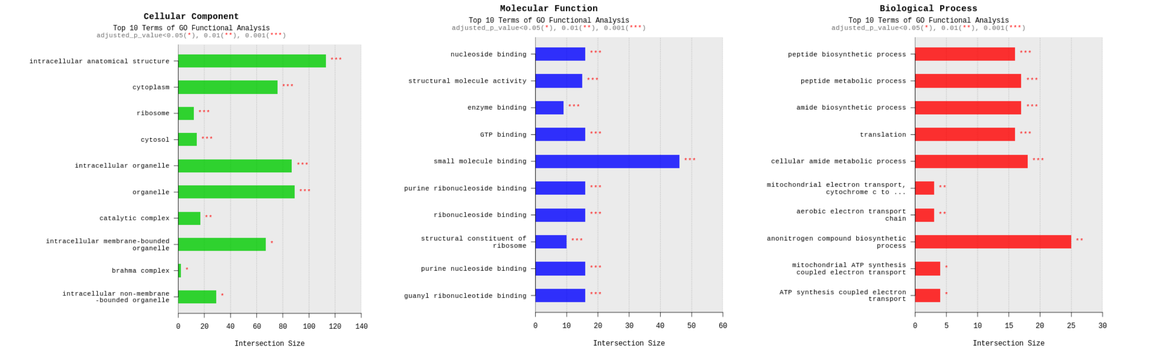

PITA+TOFO12W vs HFD 12W

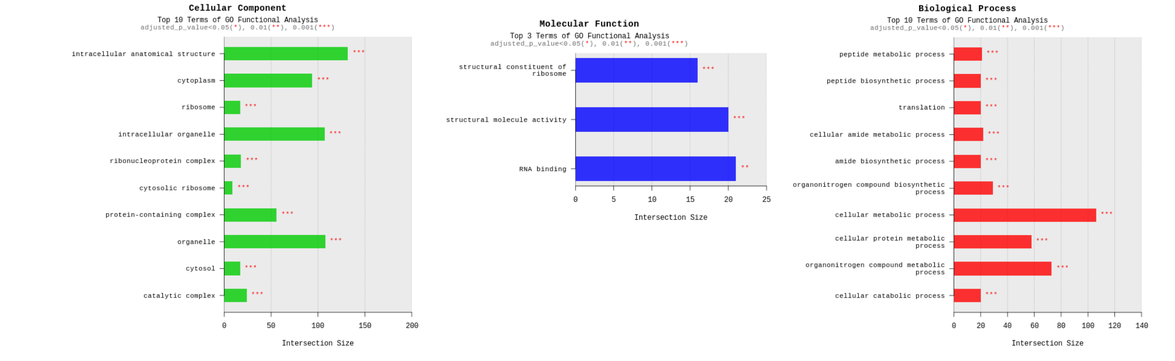

Supplementary Figure 3

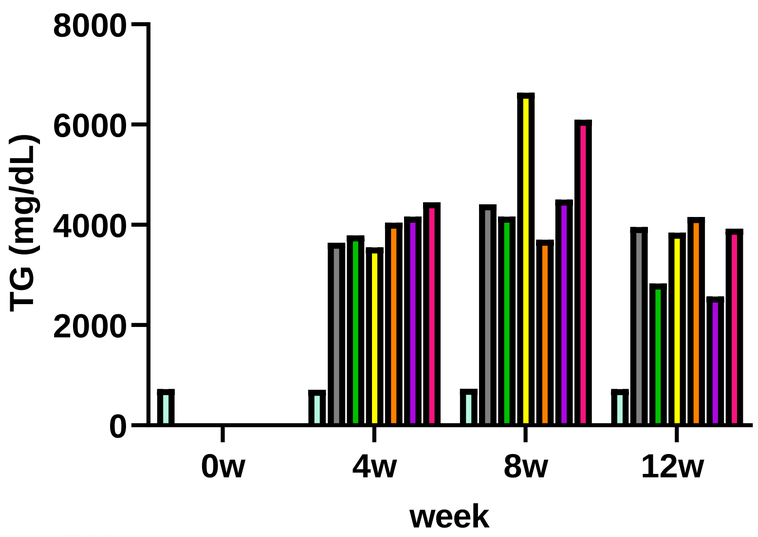

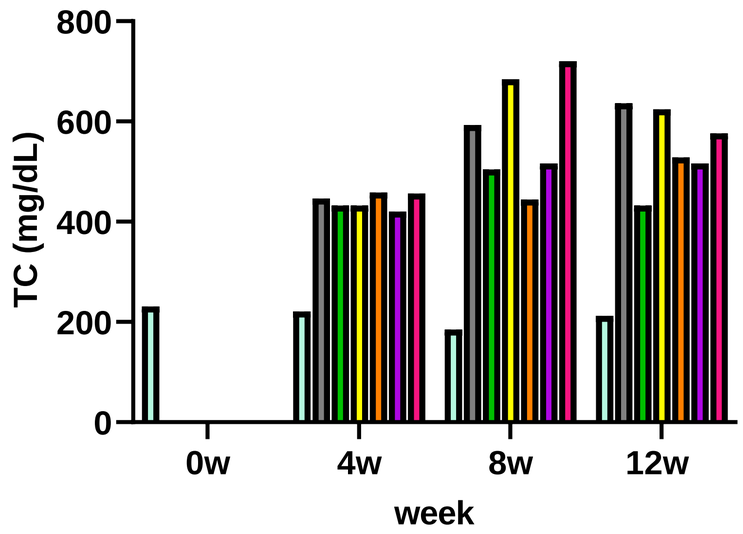

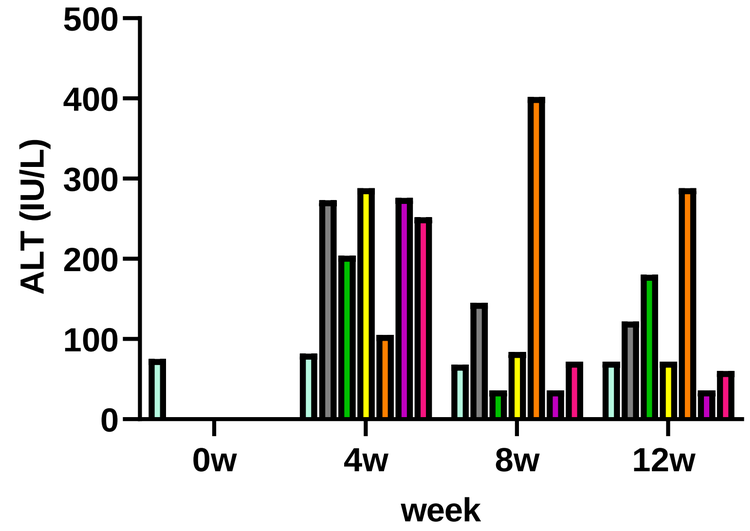

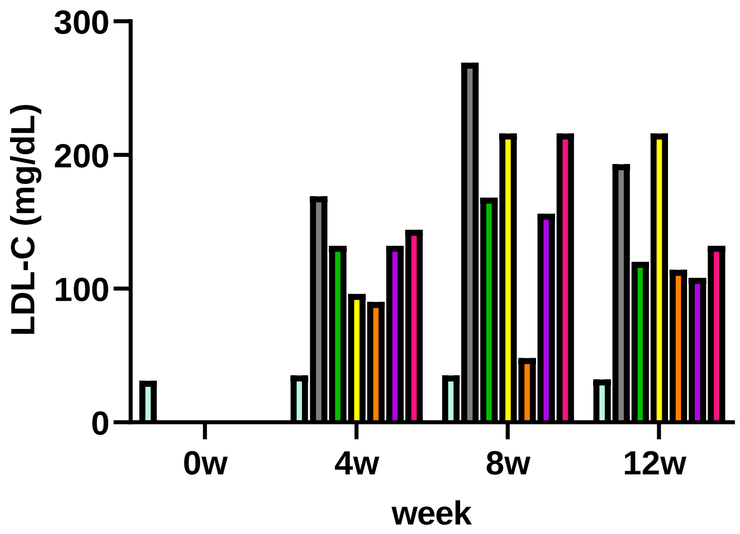

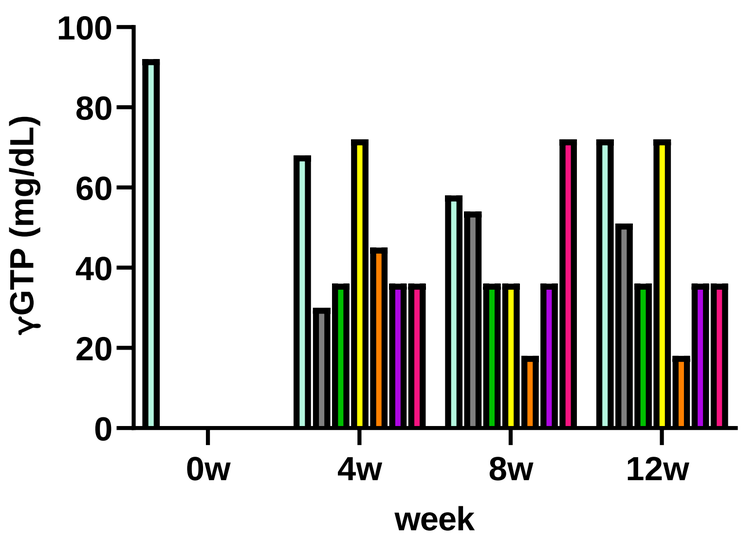

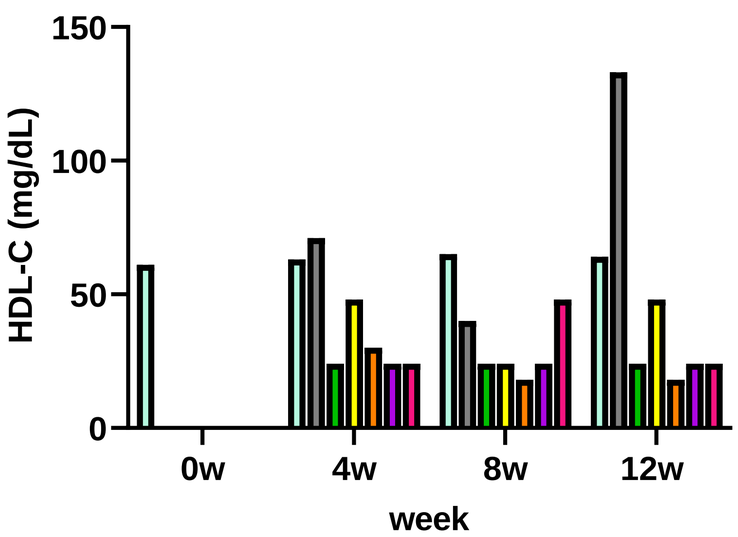

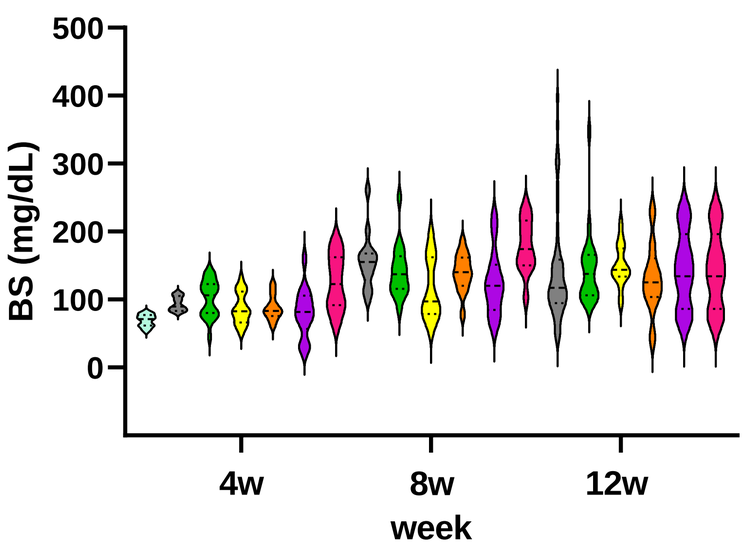

Supplementary Table 1.

Gapdh F	ACCTCCACTCCACCTAAGCA
Gapdh R	GCTTCATGCACTGGAAGACA
Col1a1a F	AAGAAGCACGTCTGGTTTGG
Col1a1a R	AAACAGACGGGTCCAACTTC
Mmp2 F	ACTGAGGGCAGAGATGATGG
Mmp2 R	TTTCAGGGCAGAAGCCATAG
Timp2b F	AGTTCTGACCCCAACATCG
Timp2b R	GCCGTCCTACCAATTTTGC
Tgfb1 F	AAGTGGCTGTCCTTTGACG
Tgfb1 R	TATCCGCTTCTTCTCCATCC
Acc1 F	GAGTGACGTCCTGCTTGACA
Acc1 R	ACCTTTGGTCCACCTCACAG
Fas F	GACGCTTCAGGAAATGGGTA
Fas R	GGACAGGAACCGGACTATCA

Pparγ F	ACGCTTCCATTTCCTCCTCT
Pparγ R	GACAGTGAAGGTCGCAGTGA
Pparα F	GCACGTCGGTGGAGACGGTCA
Pparα R	CTTTGGCTCCATCATGTCGC